Fluorescence Lifetime Heterogeneity in Aggregates of LHCII Revealed by Time-Resolved Microscopy

Virginijus Barzda,* Cees J. de Grauw,[†] Jurrien Vroom,[†] Foske J. Kleima,* Rienk van Grondelle,*
Herbert van Amerongen,* and Hans C. Gerritsen[†]

*Faculty of Sciences, Department of Physics and Astronomy, Vrije Universiteit Amsterdam, 1081 HV Amsterdam, The Netherlands; and
[†]Debye Institute, Utrecht University, 3508 TA Utrecht, The Netherlands

ABSTRACT   Two-photon excitation, time-resolved fluorescence microscopy was used to investigate the fluorescence quenching mechanisms in aggregates of light-harvesting chlorophyll *a/b* pigment protein complexes of photosystem II from green plants (LHCII). Time-gated microscopy images show the presence of large heterogeneity in fluorescence lifetimes not only for different LHCII aggregates, but also within a single aggregate. Thus, the fluorescence decay traces obtained from macroscopic measurements reflect an average over a large distribution of local fluorescence kinetics. This opens the possibility to resolve spatially different structural/functional units in chloroplasts and other heterogeneous photosynthetic systems in vivo, and gives the opportunity to investigate individually the excited states dynamics of each unit. We show that the lifetime distribution is sensitive to the concentration of quenchers contained in the system. Triplets, which are generated at high pulse repetition rates of excitation (>1 MHz), preferentially quench domains with initially shorter fluorescence lifetimes. This proves our previous prediction from singlet-singlet annihilation investigations (Barzda, V., V. Gulbinas, R. Kananavicius, V. Cervinskas, H. van Amerongen, R. van Grondelle, and L. Valkunas. 2001. *Biophys. J.* 80:2409–2421) that shorter fluorescence lifetimes originate from larger domains in LHCII aggregates. We found that singlet-singlet annihilation has a strong effect in time-resolved fluorescence microscopy of connective systems and has to be taken into consideration. Despite that, clear differences in fluorescence decays can be detected that can also qualitatively be understood.

INTRODUCTION

Light harvesting is one of the most important steps in the use of solar energy by photosynthetic organisms. The task is accomplished by a complex structure of numerous pigment-protein complexes hosting many chlorophyll and carotenoid molecules. Light excitation, which is preferentially absorbed by the light-harvesting antenna, migrates toward the reaction center where charge separation takes place. Information about the dynamics of excited states can be obtained from ultrafast laser spectroscopy experiments. However, measurements on these complex heterogeneous structures give an averaged kinetics in experiments in bulk samples (Van Grondelle et al., 1994). The acquired data must then be decomposed into several spectral/temporal components that are assigned to certain structural features of the system under investigation (Van Stokkum, 1997; Gradinaru et al., 1998; Connelly et al., 1997). A classical example is the multiexponential fluorescence decay of photosystem two (PSII) membranes, which was attributed to the presence of different (α and β) reaction centers (Roelofs et al., 1992). Time-resolved fluorescence microscopy offers a new opportunity to investigate the excited-state dynamics in different parts of photosynthetic systems.

Time-resolved fluorescence microscopy can be performed on a single microvolume (voxel) with a near-field (for a review see Xie and Trautman, 1998) or far-field technique (for comparison of near- and far-field microscopy see Trautman and Macklin, 1996). In fluorescence lifetime imaging (FLIM), the far-field fluorescence decay is recorded with a scanning microscope and image is constructed from the fluorescence lifetime values obtained for each voxel of the scanned field (for review see Draaijer et al., 1995). FLIM exploits the differences in fluorescence lifetimes of the molecules in the sample as a contrast mechanism (Morgan et al., 1990; Buurman et al., 1992). FLIM is independent of factors like concentration of chromophores in the voxel, reabsorption effects, and fading due to photobleaching, which can strongly influence fluorescence intensity images.

Fluorescence lifetimes of individual photosynthetic pigment-protein complexes were measured on light-harvesting complexes of LH-2 from *Rhodopseudomonas acidophila* and showed that at room temperature initially all molecules possessed very similar monoexponential fluorescence decay. The decays corresponded to the macroscopically measured kinetics, and only after some time of illumination did molecules switch to different quenching states with different lifetimes (Bopp et al., 1997). A more complicated situation is expected in complex systems like aggregates of pigment-protein complexes, chloroplasts, or thylakoid membranes, where many complexes and quenching centers are present in the system. In such systems, in addition to different pigment-protein complexes, connectivity diversifies the fluorescence lifetimes due to the lifetime depen-

dence on the size of the domain (a domain is defined as an area of the system in which excitation migrates during its lifetime) and the concentration of the quenchers in the domain (see Discussion). However, even with the obvious presence of structural and lifetime heterogeneity in the complex systems, the microscopic investigations may fail to resolve lifetime differences in some systems because diffraction-limited focal volume is rather large compared to the individual pigment-protein complexes and all heterogeneity might be contained in a single voxel, but may not show up between the voxels. In the systems where differences between the voxels can be resolved, time-resolved fluorescence microscopy comes up as a powerful tool for dynamic, structural, and functional noninvasive investigations of complex photosynthetic systems.

Pioneering time-resolved microscopic studies were performed on several complex photosynthetic systems. Near-field time-resolved fluorescence measurements on a single location in photosynthetic membrane from a mutant of *Chlamydomonas reinhardtii* containing mainly aggregated light-harvesting pigment-protein complexes of photosystem II (LHCII) showed a biexponential fluorescence decay with similar lifetimes but different amplitudes as compared to the macroscopic measurements (Dunn et al., 1994). This suggested the presence of lifetime heterogeneity even inside the voxel, which is below the diffraction limit. FLIM measurements of chlorophyll (Chl) containing polyvinyl alcohol matrices revealed heterogeneity of fluorescence lifetimes between the voxels, and fluorescence quenching centers could be resolved (Sanders et al., 1996). FLIM was also used to discriminate between the chloroplasts and cell membrane of the alga *Gymnodinium nagasakience* (Draaijer et al., 1995). In this study we investigate the spatial heterogeneity of fluorescence decay kinetics in aggregates of LHCII by means of FLIM and individual microvolume time-resolved fluorescence.

LHCII aggregates are structurally well characterized (Simidjiev et al., 1997) and the crystal structure of LHCII is known at 3.4 Å resolution (Kühlbrandt et al., 1994). Several pigment-protein complexes with distinct apoprotein isoforms and altered Chl *a*, Chl *b*, and carotenoids (Cars) composition constitute LHCII (for a recent review see Sandoná et al., 1998). In vivo, LHCII is found in a trimeric form or in a heptameric association of trimers (Dekker et al., 1999). Electron microscopy studies on partially solubilized thylakoid membranes showed several specific locations of LHCII trimers in supramolecular organization of PSII (Boekema et al., 1999).

Ultrafast pump-probe and three-pulse photon echo studies on trimeric LHCII show that spectral equilibration completes within ~10 ps after laser excitation (Gradinaru et al., 1998; Agarwal et al., 2000). The decay of the spectrally equilibrated state in detergent-solubilized LHCII is dominated by a 3.6-ns component as revealed by the fluorescence kinetics at room temperature (Connelly et al., 1997). Ag-

gregation of isolated LHCII induces remarkable fluorescence quenching and the appearance of heterogeneous fluorescence decays with several lifetimes in the range of hundreds of picoseconds (Mullineaux et al., 1993). The fluorescence decay of aggregates is also shortened by light-induced quenchers that can disappear in the dark (Jennings et al., 1991; Barzda et al., 2000). The fluorescence decay appears to be distorted by singlet-singlet or singlet-triplet annihilation if the excitation intensity is too high (Valkunas et al., 1991). Singlet-singlet annihilation usually becomes significant under high light intensities when more than one excitation is present in the same domain. For LHCII aggregates the annihilation takes place from several picoseconds to many hundreds of picoseconds (Barzda et al., 1996, 2001).

Lifetime images obtained in this work show that large heterogeneity in the fluorescence lifetimes exists not only for different LHCII aggregates, but even within one single aggregate. Fluorescence lifetimes that are measured in the bulk sample can be understood as characteristic (average) lifetimes of the large distribution of the microscopic values. We show that the lifetime distribution is sensitive to the concentration of the quenchers contained in the system. By using the singlet-triplet annihilation phenomena in FLIM, we can obtain structural information on the fluorescence quencher distribution in various sizes of the domains, which is important for understanding excitation migration and fluorescence quenching mechanisms in light-harvesting antenna. This study also provides a basis for further FLIM investigation on individual thylakoid membranes, chloroplasts, and other complex photosynthetic systems in vivo.

MATERIALS AND METHODS

Sample preparation

LHCII was isolated from dark-adapted leaves of two-week-old pea (*Pisum sativum*) plants as described in Simidjiev et al. (1997). LHCII was purified several times by solubilization of aggregates (Chl $a+b$ concentration of 1 mg/ml) with 0.1% (w/v) n-dodecyl β-D-maltoside (DM) in 10 mM Tricine/KOH, pH 7.6, buffer and subsequent aggregation with 20 mM of Mg_2Cl and 100 mM KCl. Aggregated LHCII was sedimented by centrifugation at $5000 \times g$ for 10 min and resuspended in 10 mM Tricine buffer. The average fluorescence lifetime increased with each purification step (Barzda et al., 1998a). Three to five purification steps were performed until a Chl a/b ratio of <1.25 was obtained. Samples were stored at 4°C and were used within two weeks after isolation. It was observed that freezing of LHCII or keeping it in the refrigerator for more than two weeks influences the fluorescence lifetimes. For microscopic investigations, LHCII aggregates, suspended in Tricine buffer (pH 7.6) containing 40% glycerol, were deposited on a microscope glass, covered with a coverslip, and left for 30 min to sediment on the glass surface.

Time-correlated single-photon counting

"Macroscopic" fluorescence lifetimes of LHCII aggregates were measured in a 1-cm cuvette with the time-correlated single photon counting (TCSPC) technique (O'Connor and Philips, 1984). Excitation light at 593 nm was

provided by a cavity-dumped dye (Rhodamine 6G) laser (Coherent 700 dye laser with 7220 cavity dumper) synchronously pumped with the second harmonic from an Nd:Yag laser (Antares 76-S, Coherent, Palo Alto, CA). Laser pulses of 8 ps at 124 kHz repetition rate were used for sample excitation. Detection was done with a microchannel plate photomultiplier (MCP PMT, R1564U-07, Hamamatsu, Japan). The instrument response time of the setup was 80 ps (FWHM). Traces were recorded under annihilation-free conditions, and the generation of light-induced fluorescence quenchers (Barzda et al., 2000) was negligible at the excitation energies below 1 nJ/pulse.

Microscope

The microscopic investigations were performed with a two-photon excitation microscope, which is described in detail elsewhere (Sytsma et al., 1998) and will be explained briefly here. The excitation was provided by a mode-locked titanium-sapphire laser (Tsunami, Spectra Physics, Mountain View, CA), which produced 80-fs pulses at 800 nm and which resulted in two-photon excitation at 400 nm in the focus of the high numerical aperture objective (water-immersion objective, 60× NA 1.2 plan-apochromatic, Nikon, Japan). The repetition rate of the laser was set between 82 MHz and 800 Hz with the pulse picker (Spectra Physics, 3980). The excitation light was scanned over the objective aperture. The fluorescent light was collected by the same objective, descanned, and directed toward a detector operating in the photon counting mode. The remaining excitation light was blocked by two 750-nm interference short-pass filters (Optosigma, Santa Ana, CA) placed in front of the detector. No pinhole was used, allowing wide-field detection of the fluorescence light. The spatial resolution of the microscope was 0.27 μm in the lateral direction and 0.67 μm in the axial direction (De Grauw et al., 1999). The pulse energy of the laser was attenuated by a set of neutral density filters to (0.2 ± 0.01) nJ/pulse for lifetime imaging (Figs. 1 and 4) and to (0.48 ± 0.05) nJ/pulse for microvolume fluorescence decay measurements (Fig. 2). When the excitation beam was scanned over the sample (Fig. 3), an excitation pulse energy of (0.88 ± 0.01) nJ/pulse was used. The average laser power on the sample was held well below 1 mW. The maximum detected photon count rate was below 10 kHz in all measurements.

Lifetime imaging

In fluorescence lifetime imaging, fluorescence decay is recorded for every pixel in the sample. The fluorescence photons were measured with an avalanche photodiode (APD, SPCM-AQ, EG&G, Canada), which gave high sensitivity and 400-ps (FWHM) time response of the setup. The photon counts from the detector were collected by a time-gating module with four different time gates, which were opened sequentially for a certain period of time after each laser pulse. The widths of the four time gates were set to 1 ns, 1 ns, 3 ns, and 5 ns (De Grauw and Gerritsen, submitted for publication). The first time gate was opened 0.7 ns after the laser excitation and there were no delays between the end of the preceding and the beginning of the following gate. The photon counts were accumulated for each pixel during a pixel-dwell time, which was set in the range between 50 μs/pixel and several thousand microseconds/pixel. Sample images of 256 × 256 pixels were recorded. For each pixel in the image, the numbers of counts in the four time gates were fitted to a single exponential using a Levenberg-Marquardt least-square fit. This resulted in the lifetime image containing the mean lifetime of each pixel. The same algorithm was used for fitting the time (t)-dependent number of counts (I) of each pixel with a double exponential:

$$I(t) = A_1 e^{-t/\tau_1} + A_2 e^{-t/\tau_2} \qquad (1)$$

The individual amplitudes (A_1, A_2) and lifetimes (τ_1, τ_2) of the exponentials could be chosen to fit freely or were set at fixed predefined values. When both lifetimes were fixed, the image was constructed from the normalized amplitudes (*A*) expressed in percentage as follows:

$$A = \frac{A_1}{A_1 + A_2} \cdot 100 \qquad (2)$$

Time-correlated single-photon-counting microscopy

Fluorescence decays from individual microvolumes of the sample were measured with the microscope by using TCSPC (O'Connor and Philips, 1984). The excitation beam was kept at the selected place or scanned over the desired area of the sample during the collection time of the photons. In these measurements the MCP PMT was used for detection. The time response of the microscope was 65 ps. This response was measured using urea crystals as a sample that produces an instantaneous, frequency-doubled emission from the applied laser pulses. The fluorescence lifetimes were determined by fitting the TCSPC decay curves with a sum of exponential terms convoluted with the instrument response using an iterative nonlinear least-square algorithm.

RESULTS

Lifetime imaging

The fluorescence lifetime imaging of LHCII aggregates was carried out with the laser scanning fluorescence microscope using two-photon excitation (Denk et al., 1990). The basic wavelength of excitation was 800 nm, which resulted in exciting the Soret band of Chl *a* at 400 nm. The fluorescence intensity image of LHCII aggregates is presented in Fig. 1 *A*. It can be seen that LHCII is aggregated into clusters of different sizes ranging from hundreds of nanometers to a few microns. The fluorescence intensity emitted from different aggregates or different parts of the same aggregate varies over a broad range. The excitation intensity of the laser was stable during the recording of the image; thus variation in the fluorescence intensity can be due to different concentration of LHCII in the different voxels and/or due to differences in the fluorescence lifetimes (and thus in the fluorescence yields) in different locations of the aggregates. Recording the image of fluorescence lifetimes as presented in Fig. 1 *B* can distinguish between the two effects. The average lifetime for each pixel of Fig. 1 *B* is obtained by fitting the amounts of counts from four time gates with a single exponential decay (see Materials and Methods). To filter out background with low count levels we present only those pixels in which the amount of photon counts was larger in the first time gate than in the second. In addition, pixels are rejected if <16 photon counts were collected in one of the first two time gates. Those "rejected" pixels are presented in black in the image. The image in 1 *B* reveals large inhomogeneities in the fluorescence lifetimes of LHCII aggregates. It shows that lifetime differences do exist not only between the aggregates, but also inside the same aggregate. Pixels with a lifetime of ~0.8 ns appear most frequently in the image. Longer lifetimes,
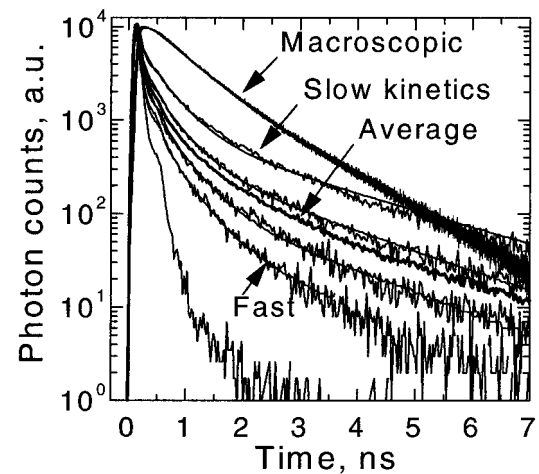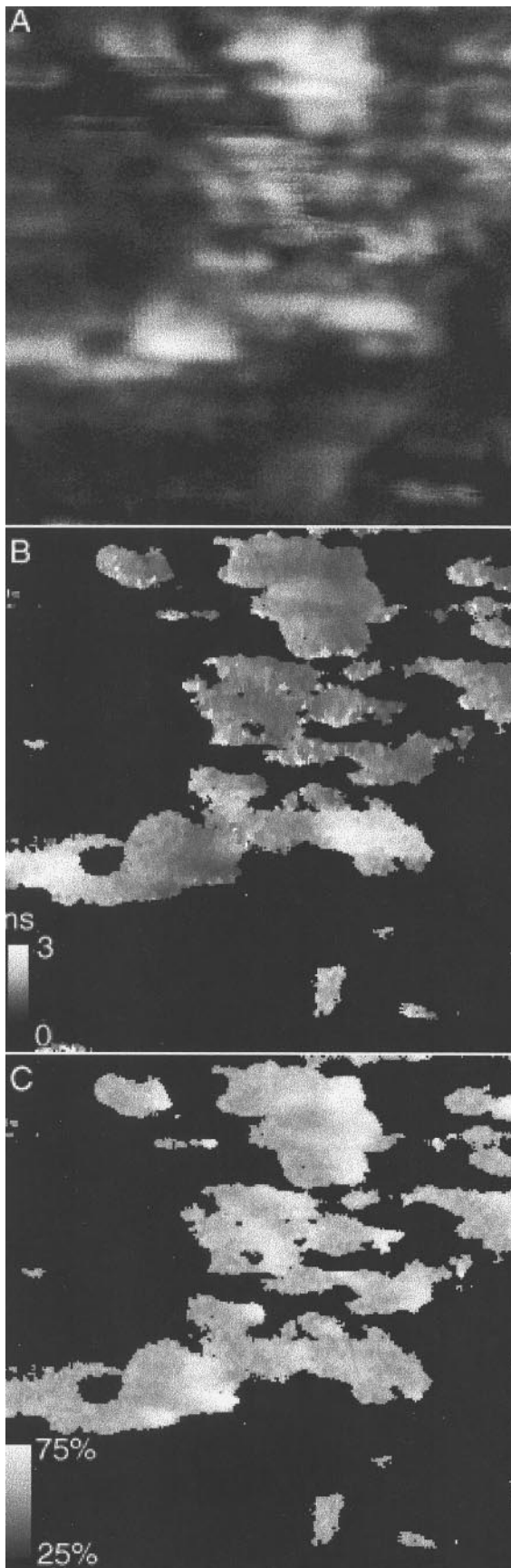
FIGURE 2   TCSPC traces from selected spots in various LHCII clusters of Fig. 1 and a TCSPC trace recorded in a macroscopic measurement. The average trace (*thick line*) was obtained by summing all the microscopic fluorescence decays measured in the same aggregate. Thin lines are multiexponential fits to the experimental traces. The fitting parameters of the labeled traces are shown in Table 1. The fastest kinetics is the instrument response of the microscopic measurement.

FIGURE 1   (*A*) Intensity image (sum of all four time gates) of LHCII clusters measured at a laser repetition rate of 80 kHz. Image size is 11 × 11 μm. More photon counts are presented in light shades, 0 photon counts are presented in black. (*B*) Corresponding lifetime image showing the fitted single exponential lifetime (for fitting details see Materials and Methods). Lifetime scale is 0–3 ns (black to white). Pixels are also presented in black when <16 counts are collected in one of the first two time gates or the number of counts in the second time gate is larger than in the first time gate. (*C*) Percentage of the 0.9-ns component (*A*, Eq. 2) of a double exponential fit (Eq. 1) with fixed lifetimes of 0.9 ns and 1.7 ns.

between 1 and 2 ns, are less frequent. Lifetimes shorter than 0.7 ns could not be resolved accurately. This is due to the response time of the avalanche photodiode, the start of the first time gate at 0.7 ns after excitation, and the width of the first two gates, which was 1 ns.

We also analyzed the time-gated images with two-exponential fluorescence decay fits (Eqs. 1 and 2). The characteristic fluorescence lifetimes were obtained by fitting the averaged fluorescence kinetics obtained from the four time-gated images. The average trace was constructed from the amounts of photon counts summed over each time-gated image and assigned to the times corresponding to delay times of each gate plus half of the width of that time gate. The fit resulted in two lifetimes of 0.9 and 1.7 ns. These two lifetimes were used to fit the fluorescence decays obtained from the time-gated photon counts at each pixel of the image. The LHCII image created from the fitted amplitude of the 0.9-ns lifetime component is presented in Fig. 1 *C*. The amplitude of each pixel is given as a percentage where the sum of the amplitudes of the two components is scaled to 100% (Eq. 2). The image in Fig. 1 *C* shows that both
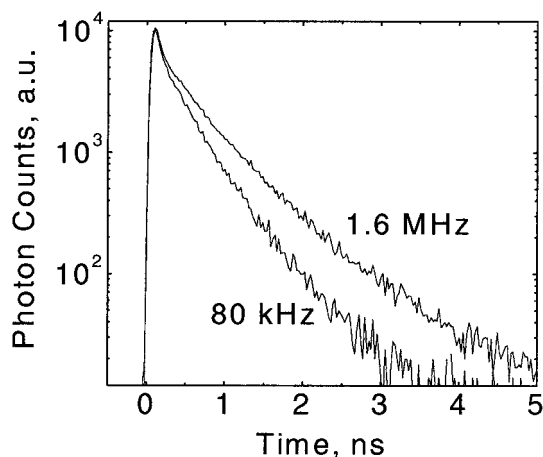
FIGURE 3 TCSPC traces acquired with 1.6-MHz and 80-kHz laser-repetition rates. Traces were measured while scanning over the LHCII clusters (30 × 30 μm area).

lifetime components are present in all LHCII aggregates, and pixels with only one component were not observed. The image reveals distinct areas with different contributions from the shorter lifetime component. The minimum percentage of the 0.9-ns component found in the image is 56%. This means that this component dominates throughout the clusters. A more detailed kinetic analysis can be achieved by recording fluorescence decay traces of individual microvolumes in the sample.

Fluorescence decay kinetics in individual microvolumes

The inhomogeneity of the fluorescence decays in LHCII aggregates was further investigated by obtaining TCSPC traces from individual microvolumes of $270 \times 270 \times 670$ nm^3 size. The traces, which are shown in Fig. 2, were taken from different spots of the LHCII aggregates located within the area of the specimen shown in Fig. 1. For comparison, a fluorescence decay trace measured in a cuvette (macrovolume) with very low excitation intensity is also shown in Fig. 2. As can be seen from the figure, all decays measured in the distinct microvolumes are different and the noise is

smaller than the differences between the traces. This proves that we are dealing with a distribution of lifetimes in Fig. 1 and not with the appearance of different lifetimes due to the low statistical number of photon counts in each pixel.

The fitted lifetimes of the decays shown in Fig. 2 are listed in Table 1. The fitted parameters of the fluorescence decays measured in the microvolumes can be compared with the decay recorded from the macrovolume (Table 1). Very fast decay components, in the order of the system response time, were found in the microvolume traces but not in the "macroscopic" measurement. Those components are attributed to singlet-singlet annihilation, which takes place under high-intensity excitation conditions when more than two excitations appear in the same domain; the domain size is determined by the excitation diffusion radius during the lifetime of the excitation. For two-photon microscopy, we have to use high intensities of the laser pulses to obtain high-quality images in a reasonable time; thus singlet-singlet annihilation will be hardly avoidable in the imaging of connective systems. In the areas where the kinetics are comparable to the instrument response time (see very fast trace in Fig. 2), domains must be present where almost all excitations annihilate. During the time-gated lifetime imaging (as in Fig. 1) the effect of annihilation is minimized by starting the first time gate of the photon counting 0.7 ns after the laser excitation. The longer-lived fluorescence components found in the microvolumes are in the range from 0.5 to 1.9 ns and are comparable to the lifetimes measured in the macrovolume or obtained from the two exponential fits of the time-gated images (see explanation of Fig. 1 C). A slightly smaller value of 0.5 ns in the microvolume measurements when compared to the 0.7 ns time in the macrovolume experiments appears to be due to the singlet-singlet annihilation and/or due to the generation of light-induced quenchers (Jennings et al., 1991; Barzda et al., 1999). More light-induced quenchers are accumulated in the microvolume during TCSPT measurements due to the much longer exposure time when compared to the dwell time of the pixel in time-gated imaging. In several microvolumes, showing slow fluorescence decay curves, a 2.8–3.0-ns component with very small amplitude was observed. Similar lifetimes

TABLE 1 Fitted lifetime components to the curves in Fig. 2

Macroscopic Measurement		Microscopic Measurement					
		Fast Kinetics		Slow Kinetics		Average Kinetics*	
A (%)	τ (ns)	A (%)	τ (ns)	A (%)	τ (ns)	A (%)	τ (ns)
		96%	annihilation[†]	85%	annihilation	92%	annihilation
87%	0.71	4%	0.55	11%	0.48	7%	0.49
13%	1.71			3%	1.9	1%	1.9
				1%	2.8		

The fluorescence lifetimes were determined by fitting the TCSPC decay curves with a sum of exponential terms convoluted with the instrument response.
*The average response was obtained by summing all the microscopic fluorescence decays measured in the same aggregate.
[†] Lifetimes shorter or comparable to the instrument response are attributed to annihilation processes.

can be found in macroscopic measurements on trimeric LHCII suspended in a buffer containing non-ionic detergent above the critical micellar concentration (Connelly et al., 1997). However, this component is not observed in the macrovolume of LHCII aggregates (Table 1). This shows that a very small amount of LHCII trimers that are not quenched during aggregation is present in the sample, but the concentration of this type of LHCII is too small to be distinguished from the noise in the macroscopic measurement of LHCII aggregates.

Effects of quenchers on the fluorescence lifetime imaging

The fluorescence quenching kinetics depends on the concentration of quenchers in a domain. We varied the concentration of the fluorescence quenchers in LHCII aggregates by inducing quenchers with a high repetition rate of excitation laser pulses. Car and Chl triplets are induced with a high quantum yield (Peterman et al., 1995; Barzda et al., 1998b) and their lifetimes are in the order of 10 μs and 1 ms, respectively. Thus at high repetition rates (>1 MHz) the triplets can be accumulated, leading to the quenching of fluorescence via singlet-triplet annihilation (Valkunas et al., 1991). In addition, Chl triplets can produce fluorescence quenchers that live up to several seconds (Barzda et al., 2000). This effect also enhances the fluorescence quenching due to accumulation of the quenchers. Fig. 3 presents fluorescence decay curves that are taken at different repetition rates of the laser. These decay curves were collected while scanning the sample over the same area of $30 \times 30 \mu$m, thus averaging the decays found in this area. The trace taken with 80 kHz repetition rate decays faster than the one recorded at 1.6 MHz. The initial part of both decay curves, which is comparable to the instrument response time, arises mainly from singlet-singlet annihilation. Apparently, at higher repetition rates more excitations are quenched at earlier times via singlet-triplet annihilation, which results in less contribution of fluorescence to the initial part of the kinetics. Normalization of the kinetics at the initial amplitude enhances the amplitudes of the slower components. Therefore, apart from the lifetime components of 0.5–0.7 ns, a component with 3 ns becomes significant at higher repetition rates.

During the time-gated lifetime imaging, counting of the photons starts after 0.7 ns, thus changes in the kinetics due to singlet-singlet annihilation do not significantly influence the imaging results (Barzda et al., 1996). In Fig. 4, an image of LHCII from a different area of the same specimen as in Fig. 1 was taken with an 8 MHz repetition rate of excitation. The image shows similar inhomogeneities to those found in Fig. 1; however, fewer short components are present. Taking an image from the same area with a different repetition rate would not allow a satisfactory comparison because permanent light-induced quenchers are induced during each
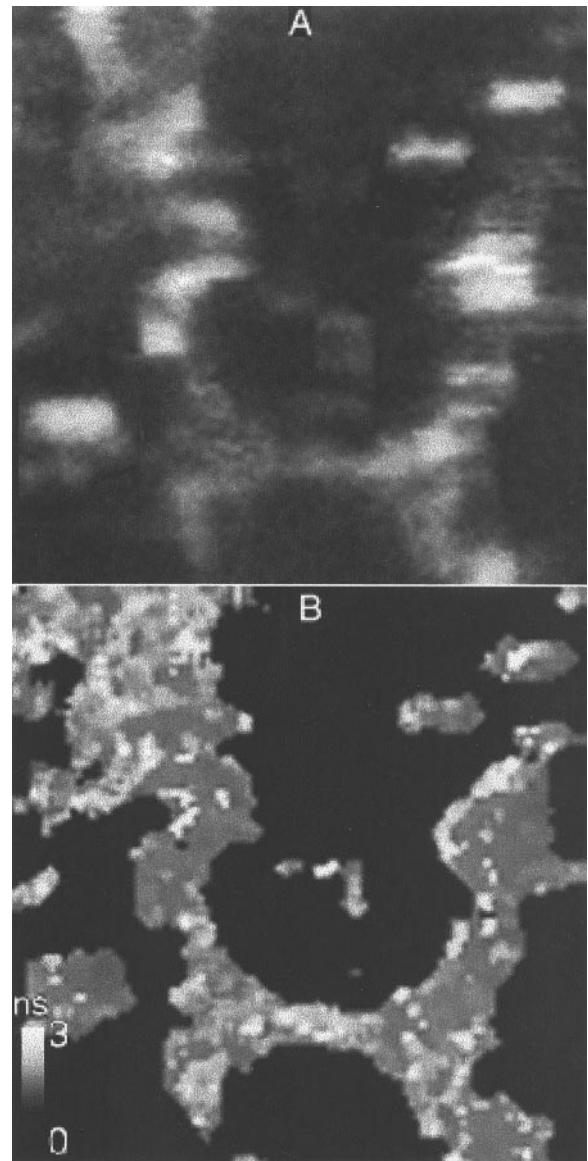

FIGURE 4 (*A*) Intensity image (sum of all four time gates) of LHCII clusters measured at a laser repetition rate of 8 MHz. Image size is 11 × 11 μm. (*B*) Corresponding lifetime image showing the fitted single exponential lifetime. Lifetime scale is 0–3 ns (black to white).

scan. In Fig. 5 we present the occurrence histogram of the lifetimes over the images shown in Figs. 1 and 4, which are taken at different repetition rates. The fluorescence decay at each pixel was fit with monoexponential kinetics. The occurrence of the lifetimes in the image was counted in a histogram with bins of 0.01 ns. At higher repetition rates the occurrence of the pixels with the shorter lifetimes is reduced; however, the occurrence of the longer lifetimes is not affected. This is in line with the expectation that more quenchers are generated at higher repetition rates. The distributions show that the quenchers are generated predominantly in the domains, which had a 0.5–0.7 ns lifetime.

A further increase of the quencher concentration can be achieved with less purified LHCII aggregates (Barzda et al.,
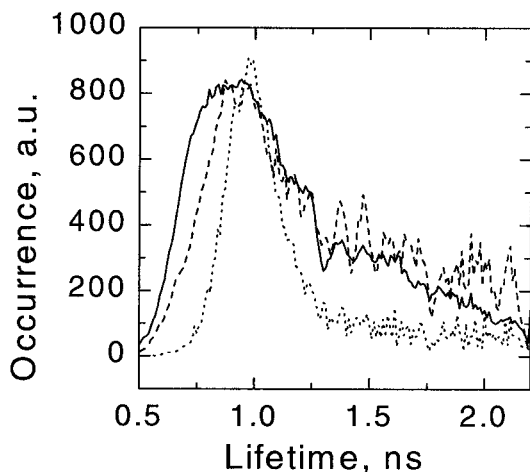
FIGURE 5 Histograms showing the distribution of monoexponentially fitted lifetimes in Fig. 1 *B* (*solid line*), Fig. 4 *B* (*dashed line*), and in the image of a non-purified sample (*dotted line*, image is not shown).

1998a). As can be seen from Fig. 5 the occurrence of pixels with short lifetimes is further reduced in the less purified LHCII sample. The amount of pixels with lifetimes longer than 1.3 ns is also reduced. The image becomes much more homogeneous with a dominating lifetime at ~0.9 ns. This most probably appears due to a homogeneous increase in the number of quenchers in all domains, which leads to the shortening of the lifetime in the domains with longer lifetimes. Generation of the quenchers in the domains with shorter lifetimes results in shortening of the lifetimes below the time resolution of our imaging system, and they do not show up in the histogram of Fig. 5.

DISCUSSION

Origin of lifetime inhomogeneity in LHCII aggregates

None of the pixels of the images showed monoexponential decay kinetics. The fluorescence lifetimes in the microvolumes varied over a broad range. Singlet-singlet annihilation cannot account for the large differences in the lifetimes on the 0.5 to 3 ns time scale because most of the annihilation in LHCII aggregates finishes after a few hundreds of picoseconds (Barzda et al., 1996). LHCII trimers show rather homogeneous lifetimes dominated by a 3.6-ns component (Connelly et al., 1997). It is known that aggregation of LHCII shortens the fluorescence lifetime, i.e., introduces quenching kinetics in LHCII aggregates (Ide et al., 1987; Ruban et al., 1992). The quenching lifetime in a spectrally equilibrated domain can be expressed as follows (Kudzmauskas et al., 1988; Valkunas et al., 1991):

$$\tau = \tau_{mig} + \tau_{trap} \tag{3}$$

where τ_{mig} is the migration or first passage time of the excitation to the trap and τ_{trap} is the trapping time. Very

often one of the two lifetimes limits the excited-state decay and one can distinguish a migration-limited and a trap-limited case. The migration time can be expressed as follows:

$$\tau_{mig} = \frac{1}{2} \frac{N}{M} f_d(N, M) \tau_{hop} \tag{4}$$

where N is the number of pigments and M is the number of traps in a domain. The $f_d(N, M)$ is a structure function of the chromophore lattice in the domain. The value of $f_d(N, M)$ depends on the number of pigments per one trap and is in the order of 0.3 to 0.8 for $N > 10$ (Kudzmauskas et al., 1988). The migration time also depends on the mean hopping time τ_{hop} between neighboring pigments.

The trapping time depends on the probability of the excitation to reside on the trap, which is M/N. It also depends on the relaxation time in the trap τ_{rel} (Pearlstein, 1982; Kudzmauskas et al., 1988; Somsen et al., 1994):

$$\tau_{trap} = \frac{N}{M} \tau_{rel} \tag{5}$$

Both the migration and trapping time depend very strongly on the number of chromophores constituting the lattice of the domain and the number of traps in the domain (Eqs. 4 and 5). The number of chromophores and traps can vary over a large range, depending on the aggregation. Thus the broad distribution in the lifetimes in our measurements is determined to a great extent by these two parameters. LHCII aggregates can have a two- or three-dimensional arrangement, or can be randomly aggregated (Simidjiev et al., 1997). This leads to different values for $f_d(N, M)$, which add to the heterogeneity of the lifetimes. The hopping time and the excitation relaxation time in the trap can also vary for different aggregates, but the hopping time is an average quantity of the aggregate, which is expected to induce only minor variations in the quenching lifetimes. The expression for τ_{rel} is rather complex and its value depends on the nature of the trap. The relaxation times characteristic for different types of traps would induce distinctive lifetimes in the fluorescence decay. In conclusion, the fluorescence lifetimes of LHCII aggregates obtained in the macroscopic measurements will reflect the average decay times of the large distribution of the "microscopic" lifetimes determined by structural parameters of the aggregates and nature of the traps.

Influence of the quencher concentration on the lifetime distribution

As stated in the previous section, the quenching lifetime depends very strongly on the domain size and the number of quenchers in the domain. In this study we varied the number of quenchers by inducing them with light or biochemically

by using less purified LHCII aggregates (Barzda et al., 1998a).

Increasing the repetition rate above the inverse relaxation time of the triplet states results in accumulation of triplets (Valkunas et al., 1991). Triplets quench the fluorescence via singlet-triplet annihilation. In addition, long-lived fluorescence quenchers are generated under strong and prolonged illumination (Jennings et al., 1991; Barzda et al., 2000). Increasing the repetition rate results in an increase of the probability to generate light-induced quenchers in domains with longer singlet state lifetimes or larger absorption cross section. In Fig. 5 we see that upon increasing the repetition rate the occurrence of long lifetimes does not change. However, there is a decrease in the occurrence of shorter lifetimes. Because the long-lived singlet states remain undisturbed, this decrease in occurrence arises from the larger domains that already contain the quenchers.

The increased number of quenchers in a less purified sample leads to a decrease in the occurrence of the shorter (0.5–0.8 ns) and longer (above 1.1 ns) lifetimes. This means that the quenchers are distributed more equally among LHCII aggregates, and aggregates have a more homogeneous structure. During purification minor pigment-protein complexes, quenchers, and membrane lipids are washed out, which apparently results in structural diversities of the aggregates and the appearance of fewer quenched and unquenched domains.

CONCLUSIONS

In the present study we used fluorescence lifetime microscopy as a spectroscopic tool for investigation of fluorescence quenching mechanisms in complex photosynthetic systems. We showed that a large lifetime distribution is present in LHCII aggregates. The observed differences in lifetimes are on a scale larger than the focal volume of a high numerical aperture objective, i.e., on a scale of hundreds of nanometers. This implies that fluorescence lifetimes are averaged out in the macroscopic measurements. Therefore, spatial distribution of fluorescence lifetimes has to be considered in macroscopic time-resolved investigations, and FLIM needs to be applied to heterogeneous samples.

We showed that the lifetime distribution is sensitive to the concentration of the quenchers contained in the system. With the use of singlet-triplet annihilation phenomena in FLIM we were able to obtain structural information on the fluorescence quencher distribution in various sizes of the domains, which is below the resolution of a light microscope. In addition, we found that singlet-singlet annihilation has a strong effect in FLIM of connective systems and has to be taken into consideration. Despite that, clear differences in fluorescence decays can be detected that can also qualitatively be understood.

The presented data are important for understanding aggregation and light-dependent fluorescence quenching mechanisms, which in turn are functionally important for the regulation of light harvesting in photosynthetic organisms. This study provides a good basis for investigations of fluorescence quenching in individual thylakoid membranes, chloroplasts, and other photosynthetic systems in vivo. It gives us a promising chance to map and research the dynamics of different (possibly α and β) PSII reaction centers in the grana of individual chloroplasts.

REFERENCES

Agarwal, R., B. P. Krueger, G. D. Scholes, M. Yang, J. Yom, L. Mets, and G. R. Fleming. 2000. Ultrafast energy transfer in LHC-II revealed by three-pulse photon echo peak shift measurements. *J. Phys. Chem.* 104:2908–2918.

Barzda, V., G. Garab, V. Gulbinas, and L. Valkunas. 1996. Evidence for long-range excitation energy migration in macroaggregates of the chlorophyll a/b light-harvesting antenna complexes. *Biochim. Biophys. Acta.* 1273:231–236.

Barzda, V., V. Gulbinas, R. Kananavicius, V. Cervinskas, H. van Amerongen, R. van Grondelle, and L. Valkunas. 2001. Singlet-singlet annihilation kinetics in aggregates and trimers of LHCII. *Biophys. J.* 80:2409–2427.

Barzda, V., R. C. Jennings, G. Zucchelli, and G. Garab. 1999. Kinetic analysis of the light-induced fluorescence quenching in light-harvesting chlorophyll a/b pigment-protein complex of photosystem II. *Photochem. Photobiol.* 70:751–759.

Barzda, V., E. J. G. Peterman, R. van Grondelle, and H. van Amerongen. 1998b. The influence of aggregation on triplet formation in light-harvesting chlorophyll a/b pigment-protein complex II of green plants. *Biochemistry.* 37:546–551.

Barzda, V., M. Vengris, F. Calkoen, R. van Grondelle, and H. van Amerongen. 1998a. Reversible light-induced fluorescence quenching: an inherent property of LHCII. *In* Photosynthesis: Mechanisms and Effects. G. Garab, editor. Kluwer Academic Publishers, The Netherlands. 337–340.

Barzda, V., M. Vengris, L. Valkunas, R. van Grondelle, and H. van Amerongen. 2000. Generation of fluorescence quenchers from the triplet states of chlorophylls in the major light-harvesting complex II from green plants. *Biochemistry.* 39:10468–10477.

Boekema, E. J., H. van Roon, J. F. L. van Breemen, and J. P. Dekker. 1999. Supramolecular organization of photosystem II and its light-harvesting antenna in partially solubilized photosystem II membranes. *Eur. J. Biochem.* 266:444–452.

Bopp, M. A., Y. Jia, L. Li, R. J. Cogdell, and R. M. Hochstrasser. 1997. Fluorescence and photobleaching dynamics of single light-harvesting complexes. *Proc. Natl. Acad. Sci. U.S.A.* 94:10630–10635.

Buurman, E. P., R. Sanders, H. C. Gerritsen, J. J. F. van Veen, P. M. Houpt, and Y. K. Levine. 1992. Fluorescence lifetime imaging using a confocal laser scanning microscope. *Scanning.* 14:155–159.

Connelly, J. P., M. Muller, M. Hucke, G. Gatzen, C. W. Mullineaux, A. V. Ruban, P. Horton, and A. R. Holzwarth. 1997. Ultrafast spectroscopy of trimeric light-harvesting complex II from higher plants. *J. Phys. Chem.* 101:1902–1909.

De Grauw, C. J., J. M. Vroom, H. T. M. van der Voort, and H. C. Gerritsen. 1999. Imaging properties in two-photon excitation microscopy, effects of refractive-index mismatch in thick specimen. *Appl. Optics.* 39:5995–6003.

Dekker, J. P., H. van Roon, and E. J. Boekema. 1999. Heptameric association of light-harvesting complex II trimers in partially solubilized photosystem II membranes. *FEBS Lett.* 449:211–214.

Denk, W., J. H. Stickler, and W. W. Webb. 1990. Two-photon laser scanning fluorescence microscope. *Science.* 248:73–76.

Draaijer, A., R. Sanders, and H. C. Gerritsen. 1995. Fluorescence lifetime imaging, a new tool in confocal microscopy. *In* Handbook of Biological Confocal Microscopy. J. P. Pawley, editor. Plenum Press, New York. 491–505.

Dunn, R. C., G. R. Holtom, L. Mets, and X. S. Xie. 1994. Near-field imaging and fluorescence lifetime measurement of light harvesting complexes in intact photosynthetic membranes. *J. Phys. Chem.* 98: 3094–3098.

Gradinaru, C. C., S. Özdemir, G. Demet, I. H. M. van Stokkum, R. van Grondelle, and H. van Amerongen. 1998. The flow of excitation energy in LHCII monomers: implications for the structural model of the major plant antenna. *Biophys. J.* 75:3064–3077.

Ide, J. P., D. R. Klug, W. Kühlbrandt, L. B. Giorgi, and G. Porter. 1987. The state of detergent solubilized light-harvesting chlorophyll a/b protein complex as monitored by picosecond time-resolved fluorescence and circular dichroism. *Biochim. Biophys. Acta.* 893:349–364.

Jennings, R. C., F. M. Garlaschi, and G. Zucchelli. 1991. Light-induced fluorescence quenching in the light-harvesting chlorophyll a/b protein complex. *Photosynth. Res.* 27:57–64.

Kudzmauskas, S., V. Liuolia, G. Trinkunas, and L. Valkunas. 1988. Nonlinear phenomena in picosecond spectroscopy of photosynthetic membranes. *In* Proc. V. UPS Topical Meeting. Z. Rudzikas, A. Piskarskas, and R. Baltramiejunas, editors. World Scientific Publishing, Singapore. 248–256.

Kühlbrandt, W., D. N. Wang, and Y. Fujiyoshi. 1994. Atomic model of plant light-harvesting complex by electron crystallography. *Nature.* 367: 614–621.

Morgan, C. G., A. C. Mitchell, and J. G. Murray. 1990. Nanosecond time-resolved fluorescence microscopy: principles and practice. *Trans. R. Microscop. Soc.* 90:463–466.

Mullineaux, C. W., A. A. Pascal, P. Horton, and A. R. Holzwarth. 1993. Excitation-energy quenching in aggregates of the LHCII chlorophyll-protein complex: a time-resolved fluorescence study. *Biochim. Biophys. Acta.* 1141:23–28.

O'Connor, D. V., and D. Philips. 1984. Time-correlated single photon counting. Academic Press, London.

Pearlstein, R. M. 1982. Excitation migration and trapping in photosynthesis. *Photochem. Photobiol.* 35:835–844.

Peterman, E. J. G., F. M. Dukker, R. van Grondelle, and H. van Amerongen. 1995. Chlorophyll a and carotenoid triplet states in light-harvesting complex II of higher plants. *Biophys. J.* 69:2670–2678.

Roelofs, T. A., C. H. Lee, and A. R. Holzwarth. 1992. Global target analysis of picosecond chlorophyll fluorescence kinetics from pea chloroplasts: a new approach to characterization of the primary processes in photosystem II alpha-units and beta-units. *Biophys. J.* 61: 1147–1163.

Ruban, A. V., D. Rees, A. A. Pascal, and P. Horton. 1992. Mechanism of ΔpH-dependent dissipation of absorbed excitation energy by photosynthetic membranes. II. The relationship between LHCII aggregation in vitro and qE in isolated thylakoids. *Biochim. Biophys. Acta.* 1102: 39–44.

Sanders, R., M. A. M. J. van Zandvoort, A. Draaijer, Y. K. Levine, and H. C. Gerritsen. 1996. Confocal fluorescence lifetime imaging of chlorophyll molecules in polymer matrices. *Photochem. Photobiol.* 64: 817–820.

Sandoná, D., R. Croce, A. Pagano, M. Crimi, and R. Bassi. 1998. Higher plants light harvesting proteins. Structure and function as revealed by mutational analysis of either protein or chromophore moieties. *Biochim. Biophys. Acta.* 1365:207–214.

Simidjiev, I., V. Barzda, L. Mustárdy, and G. Garab. 1997. Isolation of lamellar aggregates of the light-harvesting chlorophyll a/b protein complex of photosystem II with long-range chiral order and structural flexibility. *Anal. Biochem.* 250:169–175.

Somsen, O. J. G., F. van Mourik, R. van Grondelle, and L. Valkunas. 1994. Energy migration and trapping in a spectrally and spatially inhomogeneous light-harvesting antenna. *Biophys. J.* 66:1580–1596.

Sytsma, J., J. M. Vroom, C. J. de Grauw, and H. C. Gerritsen. 1998. Time-gated fluorescence lifetime imaging and microvolume spectroscopy using two-photon excitation. *J. Microsc.* 191:39–51.

Trautman, J. K., and J. J. Macklin. 1996. Time-resolved spectroscopy of single molecules using near-field and far-field optics. *Chem. Phys.* 205:221–229.

Valkunas, L., V. Liuolia, and A. Freiberg. 1991. Picosecond processes in chromatophores at various excitation intensities. *Photosynth. Res.* 27: 83–95.

Van Grondelle, R., J. P. Dekker, T. Gillbro, and V. Sundström. 1994. Energy transfer and trapping in photosynthesis. *Biochim. Biophys. Acta.* 1187:1–65.

Van Stokkum, I. H. M. 1997. Parameter precision in global analysis of time-resolved spectra. *IEEE Trans. Instrum. Meas.* 46:764–768.

Xie, X. S., and J. K. Trautman. 1998. Optical studies of single molecules at room temperature. *Annu. Rev. Phys. Chem.* 49:441–480.